JOURNAL OF THE KOREAN ASTRONOMICAL SOCIETY
34: S321 ~ S323, 2001

Transonic Magnetohydrodynamic Turbulence

HYESOOK LEE [1], DONGSU RYU [1], JONGSOO KIM [2], AND T. W. JONES [3]
[1] Department of Astronomy & Space Science, Chungnam National University, Daejon 305-764, Korea
[2] Korea Astronomy Observatory, 61-1, Hwaam-Dong, Yusong-Ku, Daejon 305-348, Korea
[3] Department of Astronomy, University of Minnesota, Minneapolis, MN 55455, USA
(Received Aug. 31, 2001; Accepted Nov. 15, 2001)

ABSTRACT

Compressible, magnetohydrodynamic (MHD) turbulence in two dimension is studied through high-resolution, numerical simulations with the isothermal equation of state. First, hydrodynamic turbulence with Mach number $\langle M \rangle_{\rm rms} \sim 1$ is generated by enforcing a random force. Next, initial, uniform magnetic field of various strengths with Alfvénic Mach number $M_a \gg 1$ is added. Then, the simulations are followed until MHD turbulence is fully developed. Such turbulence is expected to exist in a variety of astrophysical environments including clusters of galaxies. Although no dissipation is included explicitly in our simulations, truncation errors produce dissipation which induces numerical resistivity. It mimics a hyper-resistivity in our second-order accurate code. After saturation, the resulting flows are categorized as SF (strong field), WF (weak field), and VWF (very weak field) classes respectively, depending on the average magnetic field strength described with Alfvénic Mach number, $\langle M_a \rangle_{\rm rms} \sim 1$, $\langle M_a \rangle_{\rm rms} \geq 1$, and $\langle M_a \rangle_{\rm rms} \gg 1$. The characteristics of each class are discussed.

Key Words : methods: numerical — MHD — turbulence

I. Introduction

Magnetic field is known to grow effectively by turbulent motion (turbulent α effect) of conducting fluid, but the field strength is not amplified any more when it is large enough to affect the turbulent motion. It might be an important issue in astrophysics to pin down the critical field strength that quenches the field amplification, since the dynamo idea is directly related to the generation of large-scale magnetic fields (Kulsrud 1999). Cattaneo & Vainshtein (1991) addressed this issue by showing that, in two-dimensional incompressible simulations, turbulent transport is reduced by the magnetic fields whose energy is small compared to kinetic energy, and even further predicted the critical field strength which is inversely proportional to the squre-root of the magnetic Reynolds number. Similarly, in three-dimensional calculations, turbulent α effect is greatly suppressed by weak fields (Tao *et al.* 1993). These results are different from a conventional belief that magnetic fields can be amplified up to the equipartition value with the kinetic energy.

In this work, we relax the incompressible approximation. Capitalizing the measured Reynolds number of an isothermal MHD code (Kim et al. 1999), we revisit, in the compressible region, the critical field strength that suppresses the amplification. For this purpose, we have done two-dimensional compressible MHD simulations with high-resolutions (up to 1536^2 cells).

II. Simulations

(a) Setup

Isothermality is assumed in flows. Then, the MHD equations of an ideal gas are

$$\frac{\partial \rho}{\partial t} + \vec{\nabla} \cdot (\rho \vec{v}) = 0, \tag{1}$$

$$\frac{\partial \vec{v}}{\partial t} + \vec{v} \cdot (\vec{\nabla} \vec{v}) + \frac{1}{\rho} \vec{\nabla} (a^2 \rho) - \frac{1}{\rho} (\vec{\nabla} \times \vec{B}) \times \vec{B} = \vec{f}, \tag{2}$$

$$\frac{\partial \vec{B}}{\partial t} - \vec{\nabla} \times (\vec{v} \times \vec{B}) = 0, \tag{3}$$

with an additional constraint

$$\vec{\nabla} \cdot \vec{B} = 0, \tag{4}$$

for the absence of magnetic monopoles. a is the isothermal sound speed and set to unity. Here the units are chosen so that the factor of 4π does not appear in the equations. In our work these equations have been solved using an isothermal MHD TVD code (Kim *et al.* 1999). The resistivity working in our simulations comes solely from the truncation of the code, in order to achieve the highest possible magnetic Reynolds number, R_m.

Simulations have been performed in the computational domain, $x = [0,1]$ and $y = [0,1]$, with a periodic boundary condition. Hence, the density in the computational box is conserved, *i.e.*,$\langle \rho \rangle = \rho_0$, where $\rho_0 = 1$. $\vec{f} = f_x \hat{\vec{x}} + f_y \hat{\vec{y}}$ is the random forcing added to momentum field at every time step. Its form is as follows;

$$f_{x,y}(x,y,t) = v_{\rm amp} \cos(\omega t + \delta_t) \sin(k_x x + \delta_x) \cos(k_y y + \delta_y), \tag{5}$$

where $\omega = 2\pi$ and $k_{x,y} = \alpha \cdot 2\pi$ with $\alpha = 4$ are used. δ_t, δ_x, and δ_y are random phases within the ranges of $0 \leq \delta_t, \delta_x, \delta_y \leq \pi$. $v_{\rm amp}$ is the forcing amplitude which results in $\langle M \rangle_{\rm rms} \sim 1$ without magnetic field. Simulations have used the resolution of 512^2, 1024^2 and 1536^2.

(b) Measurement of R_m

In numerical simulations, diffusion of momentum and magnetic field across cell boundaries occurs and results in effective numerical viscosity and resistivity, respectively. To measure the numerical resistivity, we compare the decay rate of a linear Alfvénic wave in numerical simulation with the predicted one. The predicted angular frequency of Alfvénic waves is

$$\omega = \frac{i}{2}\left(\frac{\mu}{\rho_0}+\eta\right)k^2 \pm c_{\rm A}k\left[1-\frac{1}{4c_{\rm A}^2}\left(\frac{\mu}{\rho_0}-\eta\right)^2 k^2\right]^{1/2}, \quad (6)$$

where $c_{\rm A} = \sqrt{B_0^2/2\rho_0}$ is the Alfvén speed along the wave propagation direction, $k = (k_x^2 + k_y^2)^{1/2}$ is the total wavenumber and μ and η is the dynamic shear viscosity and the electrical resistivity, respectively (see Kim *et al.* 1999 for detail). The decay rate, $\Gamma_{\rm A}$, is

$$\Gamma_{\rm A} = \frac{1}{2}\left(\frac{\mu}{\rho_0}+\eta\right)k^2. \quad (7)$$

And a *Reynolds* number on Alfvénic turbulence of scale, L is defined by

$$R_m \equiv (c_A L)/\left[\frac{1}{2}(\mu\rho_0+\eta)\right] = \frac{8\pi^2 c_A}{L\Gamma_A}. \quad (8)$$

The numerical Reynolds number, R_m, is given as a function of the spatial resolution, n_{cell}, as $R_m = 2.7 \times n_{cell}^{1.66}$ (see Kim *et al.* 1999 for detail). It is almost proportional to n_{cell} as $R_m \propto n_{\rm cell}^2$ confirming the second-order nature of the code.

III. Results

(a) HD turbulence

Without magnetic field, a transonic turbulence with $\langle M \rangle \sim 1$ is fully developed. Its energy spectrum follows the statistical Kraichnan spectrum as shown Fig. 1 (Lesieur 1990). The peak at $k/2\pi = 5.7$ occurs at the input scale of the random force, k_{in}. In the range of $k \leq k_{in}$, a $k^{-5/3}$ spectrum is presented indicating the inverse energy cascade, while in the range $k > k_{in}$, a k^{-3} spectrum is shown meaning the direct cascade of enstrophy.

(b) MHD turbulence

The hydrodynamic turbulence described above has been used as the initial velocity field of magnetic cases.

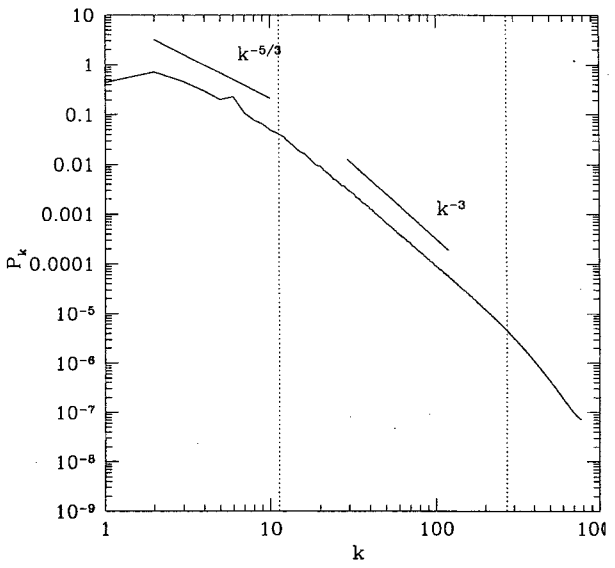

Fig. 1.— Time-averaged energy spectrum for the hydrodynamic turbulence with 1536^2 resolution. $k = \sqrt{k_x^2 + k_y^2}$. Vertical lines indicate the inertial range, which we have estimated. The figure shows that the spectrum is consistent with the Kraichnan spectrum.

Table1. Classification with different initial M_a's and different numerical resolution.

$n_{cell} \setminus M_a$	25	50	100	200	300
512^2	SF	WF	VWF	VWF	VWF
1024^2	SF	SF	WF	VWF	VWF
1536^2	SF	SF	WF	WF	VWF

We have computed a number of cases with the initial M_a ranging from 1000 to 10. The resulting flows have been classified into three classes after saturation, *i.e.*,VWF (Very Weak Field), WF (Weak Field), and SF (Strong Field) to describe the characteristics of turbulent quantities under different magnetic field strengths. The classification is shown in Table 1.

In the cases of VWF, there is virtually no magnetic field contribution to flow motion. The WF cases show the characteristics distinguished from non-magnetic case by the effects of small scale magnetic field. In the SF cases, the turbulent motion is significantly suppressed in all scales. In order to see the effects of magnetic field, we have computed the averaged turbulent quantities such as the flow velocity, $\langle v \rangle_{\rm rms}$, which is same as the mach number, $\langle M \rangle_{\rm rms}$, since isothermality has been assumed, the magnetic field strength, $\langle B \rangle_{\rm rms}$, the density contrast, $\langle \delta\rho/\rho \rangle_{rms}$, and the intermittency, $I = \langle B^4 \rangle / \langle B^2 \rangle^2$. Fig. 2 shows $\langle v \rangle_{\rm rms}$ and $\langle B \rangle_{\rm rms}$.

Cattaneo (1994) predicted that the boundary value of magnetic Reynolds number between VWF and WF cases is given as $B_c \sim {R_m}^{-1/2} v$. The square root value

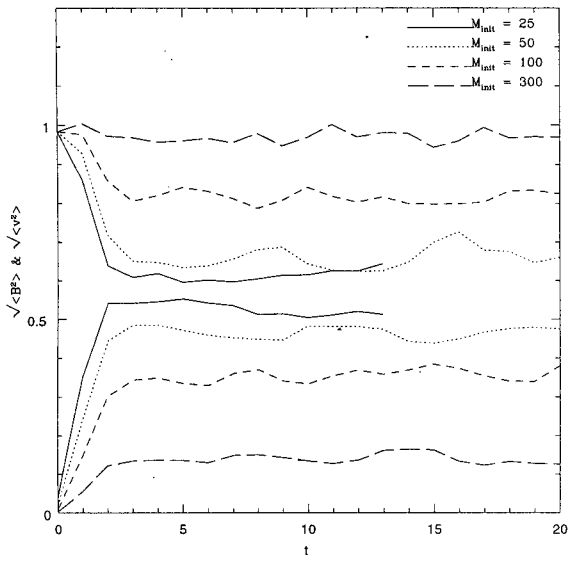

Fig. 2.— Time evolution of rms velocity and magnetic field strength for different initial Alfvén Mach numbers with 1536^2 resolution. Four lines in upper part are the evolution of rms velocity and those in lower part are that of rms magnetic field.

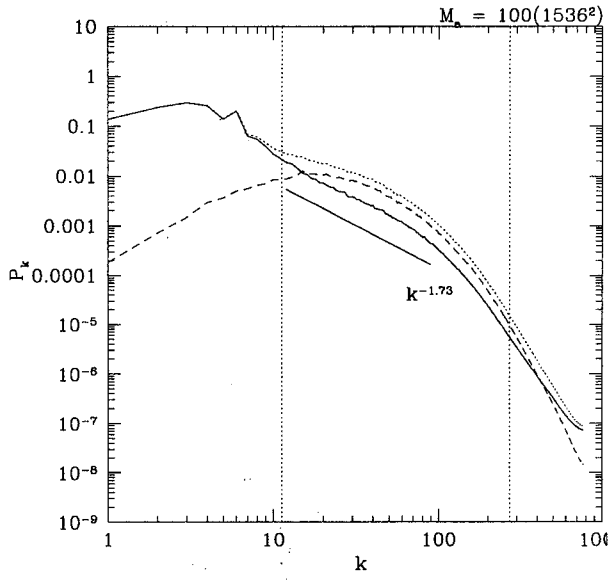

Fig. 3.— Time-averaged power spectrum for $M_a = 200$ with 1536^2 resolution. This belongs to the WF classes. Solid line - kinetic energy power spectrum, P_k^K. Dashed line - magnetic energy power spectrum, P_k^M. Dotted line - total energy power spectrum, P_k^{tot}.

of our numerical Reynolds number, $\sqrt{R_m}$, is about 92, 164, and 230 at the input scale, k_{in}, with spatial resolution, 512^2, 1024^2, and 1536^2, respectively. These are comparable to the boundary values of initial M_a between VWF and WF cases (note that out initial $\langle v \rangle_{\rm rms} \sim 1$).

In the WF cases, magnetic field is confined mostly in thin tubes with intermittency, $I \geq 3.7$. The saturated rms velocity is severely reduced even though initial $M_a \gg 1$. This is because the magnetic field in small scales suppresses fluid motions. In large wavenumber region, the power of magnetic energy exceeds that of kinetic energy ($P_k^K \lesssim P_k^M$), although in small wavenumber region, the power of kinetic energy is still greater than that of magnetic energy ($P_K^k > P_M^k$) (Fig. 3). In the SF class, magnetic field is mostly in circular shape structures with $I \leq 2.2$. The saturated rms velocity is less than $\sim$ 70% of the initial value. The power of magnetic energy exceeds that of kinetic energy in almost all $k \gtrsim k_{in}$ with the spectral slope of total energy following the Iroshnikov-Kraichnan spectrum (~ 1.5), which is expected for fully developed MHD turbulence.

IV. Conclusion

Through simulations, we have studied the suppression of turbulent diffusion under the effects of magnetic field with various strengths. The suppression could be important even when the magnetic field strength is weak. The criterion is given by $B_c \sim {R_m}^{-1/2} v$ (Cattaneo 1994).

ACKNOWLEDGEMENTS

The work by HL and DR was supported in part by KRF through grant KRF-2000-015-DS0046. Simulations have been made through the support by "The 2nd Supercomputing Application Support Program of KISTI". The work by TWJ was supported in part by NASA grant NAG5-5055, by NSF grant and AST00-71167, and by the University of Minnesota Supercomputing Institute.

REFERENCES

Cattaneo, F., and Vainshtein, S. I. 1991,ApJ, 376, L21

Cattaneo, F. 1994, ApJ, 434, 200

Kim, J., Ryu, D., Jones, T. W. and Hong, S. 1999, ApJ, 514, 506

Kulsrud, R. M. 1999, Ann. Rev. Astron. Astropys., 37, 37

Lesieur, M. 1990, Turbulence in Fluids, 2nd ed. (Dordrecht: Kluwer)

Tao, L., Cattaneo, F., and Vainshtein, S. I. 1993, in Solar and Planetary Dynamos, ed M. R. E Proctor, P. C. Matthews, & A. M. Rucklidge (Cambridge Univ. Press), p. 303